NASA TM-86700

NASA Technical Memorandum 86700

Decay of a Coherent Scalar Disturbance in a Turbulent Flow

Robert M. Kerr, Tohru Nakano, and Mark Nelkin

June 1985

National Aeronautics and
Space Administration

NASA Technical Memorandum 86700

Decay of a Coherent Scalar Disturbance in a Turbulent Flow

Robert M. Kerr, Ames Research Center, Moffett Field, California
Tohru Nakano,
Mark Nelkin, Cornell University, Ithaca, New York

June 1985

National Aeronautics and
Space Administration

Ames Research Center
Moffett Field, California 94035

Decay of a coherent scalar disturbance in a turbulent flow

ROBERT M. KERR[1]

NASA Ames Research Center
M.S. 202A-1, Moffett Field, CA 94035

TOHRU NAKANO[2] AND MARK NELKIN

School of Applied and Engineering Physics
Cornell University, Ithaca, NY 14853
November 1984

ABSTRACT. The time evolution of an initially coherent, sinusoidal passive-scalar disturbance is considered when the wavelength q is less than the length scale of the surrounding isotropic turbulent flow. In 64^3 direct numerical simulations a Gaussian prescription for the average scalar amplitude breaks down after a timescale associated with the wavenumber of the disturbance and there is a transition to a new characteristic decay. The Gaussian prescription is given by $exp[-\frac{1}{2}q^2w(t)]$, where a form for $w(t)$, the Lagrangian mean square displacement of a single fluid particle, is proposed. After the transition the decay is given by $exp[-t/\tau]$, where τ is the new characteristic timescale. If $q > k_k$, then $1/\tau = 1/\tau_D + 1/\tau_k$, where k_k is the Kolmogorov wavenumber, τ_D is the diffusive timescale and τ_k is the Kolmogorov timescale. For $q < k_k$, there is a transition, but the new decay has not been characterized.

An experiment originally proposed by de Gennes is considered in which the evolution of a coherent laser-induced pattern is read by a diffracting laser. The theory of this experiment involves the dispersion of particle pairs, but it is shown that in a certain limit it reduces to our single Fourier-mode problem and can be described in terms of single particle diffusion. The decay of a single mode after the transition in the simulation best describes the experiment.

1. Introduction

In many experimental situations an initially coherent, passive-scalar disturbance, $\theta(\vec{r},0)$, is added to a turbulent flow. For example, a coherent disturbance can be approximately added as a single Fourier mode through illumination (Petit & Guyon 1979; Fermiger et al. 1982; Limat 1984) or by a heated screen in a wind tunnel (Warhaft & Lumley 1978). An example of a coherent disturbance in physical space is the thermal-interface experiment of Larue & Libby (1981). The subsequent evolution of the average scalar amplitude $\theta(\vec{r},t)$, of the scalar fluctuations $\theta^2(\vec{r},t)$,

[1]Present address: L-387, Lawrence Livermore National Laboratory, P. O. Box 808, Livermore, CA 94550

[2]Permanent address: Physics Department, Chuo University, Tokyo, Japan

and scalar-velocity correlations, are of considerable interest. In the experiment of Larue & Libby (1981), a simple eddy diffusivity was able to account for the spread of the average profile. While these arguments should apply for long times over large length scales (when compared to the turbulent scales), it is not clear why they work well for disturbances within the turbulent scales.

In this paper the problem of the decay of a single Fourier mode

$$\theta(\vec{r},0) = \theta_0 cos(qx), \tag{1}$$

imposed on a decaying, isotropic, turbulent, velocity field is addressed using a mixture of simple analytic arguments and direct numerical simulation. The numerical method used is a 64^3 pseudospectral code with periodic boundary conditions. It has been shown by Herring & Kerr (1982) that for the Taylor-microscale Reynolds numbers R_λ (see eq. 10), as low as 15, a simulation such as this will exhibit values for some correlations, such as the velocity-derivative skewness (see eq. 11), which are characteristic of fully developed turbulence. The nature of the simulation and its limitations are discussed in § 2.

In § 3 we suggest that for short times the average amplitude of the decaying single mode is accurately given by

$$A(q,t) = < \theta(\vec{r},t) > = \theta_0 exp[-\frac{1}{2}q^2 w(t)], \tag{2}$$

where $w(t)$ is the Lagrangian mean-square displacement of a fluid particle. For steady turbulence this formula reduces to $w(t) \sim t$, which is the standard eddy diffusivity equation for long times and large length scales (see Tennekes & Lumley 1972, p. 230). But for short times, we show that a different approximation to the Lagrangian mean-square displacement applies. In § 4 this estimate is compared with the amplitude $A(q,t)$ of a single mode calculated by the numerical simulation. The comparison is good at short times, but the numerical results also suggest that for longer times the entire formulation breaks down and there is a transition to a different form of diffusion. We find that if the wavenumber, q, of the initial mode is less that the Kolmogorov wavenumber cutoff, k_k (see eq. 12), and greater than $\frac{1}{L}$, where L is the integral scale of the turbulence (see eq. 14), the transition will occur after a timescale associated with velocity disturbances of wavenumber q. However, if q is above the Kolmogorov wavenumber cutoff, the only velocity timescale available is the Kolmogorov timescale, τ_k (see eq. 13), and the transition occurs only after that time, almost independent of q. The subsequent decay depends only on the diffusive and Kolmogorov timescales and obeys $\theta(t_t)exp(-(t-t_t)/\tau)$, where t_t is the transition time and $1/\tau = 1/\tau_D + 1/\tau_k$. τ_D is the diffusive timescale $q^2 D$.

In § 5 our result is compared to an experiment suggested by de Gennes (1977) and since performed by Guyon and others. In this experiment an initially coherent, passive-scalar disturbance of the form

$$\theta(\vec{r},0) = \theta_0 cos(qx) S(\vec{r}) \tag{3}$$

is created by an optical flash. The envelope function $S(\overrightarrow{r})$ has a spatial extent l with $ql >> 1$. By diffraction of a laser beam from the resulting inhomogeneity in the index of refraction, the evolution of the intensity of this initial disturbance can be observed. For an idealized detector the measured quantity is

$$I(q,t) = < | \int d\overrightarrow{r} S(\overrightarrow{r}) exp\{iq[x(t) - x(0)]\}|^2 > . \qquad (4)$$

As shown by de Gennes, (4) is formally equivalent to a problem in turbulent pair diffusion. However, if the envelope length scale, l, in (4) is large compared to the integral length scale of the turbulence, then the spatial integral in (4) does all the needed averaging, and the subsequent ensemble or time average is superfluous. Under these conditions, (4) reduces to the single Fourier mode problem of § 2,3 and comparisons between our results and the experiments are possible.

The experimental method has been developed by Petit and Guyon (1979), and extended by Fermiger et al.(1982) and Limat (1984) for Poiseuille flow through a cylindrical pipe. In the experiments the Prandtl number is large and the wavenumber is above the Kolmogorov cutoff, both of which are just within the limits of our simulation. Significant differences between the experiment and simulation are that the experimental velocity field is not isotropic and that the experimental envelope length scale l is the order of q^{-1}, which implies that spatial averaging cannot be applied. Nevertheless, they find that the turbulent decay of the single mode is independent of wavenumber and characterized by τ_k, which is qualitatively similiar to our results for $Pr = 4.0$ and $q > k_k$ after the transition.

2. Numerical Method

Two numerical codes, described in Rogallo (1981) and Kerr (1985), were used to simulate the decay of single scalar modes. Both codes are three-dimensional pseudospectral codes with periodic boundary conditions. By spectral we mean that the fundamental variables which are stored and advanced in time are the Fourier-transformed velocity and scalar fields $u(\overrightarrow{k})$ and $\theta(\overrightarrow{k})$. In addition to the incompressible Navier-Stokes equations, each code can simulate any reasonable number of scalar equations. There are no significant differences between the two codes with respect to the current problem and they were used for different aspects of the problem for historical reasons. The code described in Kerr (1985) is written in Fortran and used the CRAY-1S computer at NASA Ames Research Center for the $R_\lambda \approx 45$ simulation. The time advancement was a third-order Runge-Kutta scheme (Wray 1981) and the only dealiasing performed was truncation of the wavenumbers outside a sphere of radius (N/2). With three scalars, 6.5 sec of cpu were used for each evaluation of the nonlinear terms without analysis. There are three evaluations per timestep and our simulation to t=0.35 required 48 timesteps or 1100 sec of cpu, which includes the cpu time for analysis. The eddy-turnover time (see eq. 14) for this simulation was $\tau_e = 0.48$.

The code described in Rogallo (1981) is written in Vectoral, and the CRAY-XMP computer at Ames was used for the $R_\lambda \approx 15$ simulation. The time advancement

was second-order Runge-Kutta and dealiasing is performed by using shifted grids on alternate evaluations and truncating outside a sphere of radius (4N/9). With three scalars, 4.0 sec of cpu were used per evaluation without analysis, and 800 sec of cpu for 80 timesteps were required for each simulation with three scalars, including analysis. The final time was t = 0.45 and the eddy-turnover time was $\tau_e = 0.9$.

The governing equations are the incompressible Navier-Stokes equation for the velocity and the transport equation for a passive scalar. The Navier-Stokes equation is

$$\partial u/\partial t + u \cdot \nabla u = -\nabla p/\rho + \nu \nabla^2 u \tag{5}$$

$$\nabla \cdot u = 0 \qquad \text{(incompressibility)}.$$

The nonlinear term, $u \cdot \nabla u$, can be written in several different forms which are computationally convenient: the conservative form,

$$\nabla \cdot (uu), \tag{6}$$

and the rotational form,

$$\omega \times u + \nabla \tfrac{1}{2} u^2. \tag{7}$$

The scalar equation can also be written two ways in incompressible flow: the convective form,

$$\partial \vartheta/\partial t + u \cdot \nabla \vartheta = D \nabla^2 \vartheta, \tag{8}$$

and the conservative form

$$\partial \vartheta/\partial t + \nabla \cdot u\vartheta = D \nabla^2 \vartheta. \tag{9}$$

In the absence of viscosity ν and diffusivity D the equations conserve two positive-definite quadratic invariants: the kinetic energy of turbulent fluctuations,

$$E = \frac{1}{2} < u_i u_i >,$$

and the scalar variance,

$$E_\theta = < \theta^2 >,$$

where the domain of integration is over all space. The fundamental dimensionless parameter that determines the velocity statistics is the Taylor-microscale Reynolds number

$$R_\lambda = \frac{U\lambda}{\nu}, \tag{10}$$

where U is the characteristic velocity of the turbulence

$$\frac{3}{2} U^2 = E,$$

and λ is the Taylor microscale,

$$\lambda = < u_1^{\,2} >^{1/2} / < (\partial u_1/\partial x_1)^2 >^{1/2} .$$

Kerr (1985) uses the rotational form of the Navier-Stokes equation (7) and the conservative form of the scalar equation (8). Rogallo (1981) uses the conservative form of the Navier-Stokes equation (6) and the convective form of the scalar equation (9). The minimum wavenumber of both simulations was 1.

The kinetic energy in both simulations was initialized with a

$$q^4 exp(-q^2)$$

spectrum, with the peak at $q = 4$ and the phases of individual wavenumbers chosen randomly. The velocity field was allowed to evolve until the velocity-derivative skewness,

$$S_u = \frac{< \left(\frac{\partial u_1}{\partial x_1}\right)^3 >}{< \left(\frac{\partial u_1}{\partial x_1}\right)^2 >^{\frac{3}{2}}} \quad , \tag{11}$$

was -0.40. This is near its steady-state value of about -0.5 (Kerr, 1983) and indicates that an energy cascade has begun. At this time, for the first simulation $R_\lambda = 45$ and the Kolmogorov wavenumber

$$k_k = (\frac{\epsilon}{\nu^3})^{\frac{1}{4}} = 33, \tag{12}$$

which are the largest permissible values if one wants to maintain good resolution of the velocity field on the 64^3 grid. To demonstrate how well the velocity field is resolved and how well the energy has cascaded to higher wavenumbers, kinetic-energy spectra for three times from this simulation are shown in figure 1. The times given are with respect to the time where $S_u \approx -0.4$. The Reynolds number, Kolmogorov wavenumber, and the Kolmogorov timescale

$$\tau_k = (\frac{\nu}{\epsilon})^{\frac{1}{2}}. \tag{13}$$

when $S_u \approx -0.4$, are given for each simulation in Table 1.

In figures 2 and 3, the time evolution of the energy and eddy-turnover times are given for the two simulations after $S_u \approx -0.4$. These will be used in the calculation of $f(t)$ by (24) and (26). An eddy-turnover time is defined as

$$\tau_e = L/U, \tag{14}$$

where

$$L = \frac{3\pi}{4E} \int k^{-1} E(k) dk \tag{15}$$

is the integral length scale and $U^2 = 2E/3$. L is the order of the simulation size and the energy decays as $t^{-2.8}$ in both simulations. Experimentally this exponent is 1.3 (Warhaft & Lumley 1978). Our value is higher for two reasons. First, the Reynolds numbers of our simulations are very low; they are therefore almost in the final period of decay. But more importantly, numerical simulations have a largest scale which inhibits the backward flow of energy. That is, the continual pairing of ever-larger vortices, a two-dimensional process which is also important in three-dimensions, is limited by the size of our box. Therefore, there is more energy at high wavenumbers and larger decay exponents than in experimental flows. We would not expect to see realistic decay exponents unless the mesh was at least 256^3 and the initial spectral peak of the kinetic energy was at a wavenumber greater than 8.

Once a steady state has been reached, we impose a single passive-scalar mode on top of the "turbulent" velocity field. This is similiar to what was done experimentally by Petit & Guyon (1979) when they illuminated their turbulent pipe with a pattern. The addition of the passive-scalar imposes additional resolution requirements. The relevant cutoff for Prandtl numbers ≥ 1 is the Batchelor cutoff (Batchelor 1959),

$$k_B = (\frac{\epsilon}{\nu D^2})^{\frac{1}{4}}. \tag{16}$$

In addition to the Kolmogorov wavenumber cutoff being less than the maximum wavenumber of the simulation, the Batchelor cutoff must also be less than this limit. For $Pr = 0.7$, this imposes no new limits on the Reynolds number. But to simulate higher Prandtl numbers, it is an important constraint. For $Pr = 4.0$ and $R_\lambda = 15$ in the second simulation, $k_B = 38$, which is slightly outside the resolution of the simulation. Therefore, the large Prandtl numbers used in the experiment of Petit & Guyon (1979) ($Pr \approx 100$) cannot be simulated. In the experiment, the wavenumber of the imposed scalar mode was between the Batchelor and Kolmogorov cutoffs. For simulation 2, with $Pr = 4.0$, this means q is between 19 and 31, the largest wavenumber of the simulation. Any mode placed between these limits is near the resolution limits of the simulation, which must be taken into account in the analysis of simulation 2 (§ 4).

The values of the Prandtl numbers and wavenumbers of the single modes tested are given in Table 1. For comparison with purely diffusive decay, the decay of two modes from simulation 2 with time for $Pr = 0.7$ and $R_\lambda = 15$ are plotted semilogrithmically in figure 4. The wavenumbers in each case are quite large, so for low Reynolds number, low Prandtl number, and high wavenumber, diffusive decay might be expected to dominate. Despite this, both modes initially decay much faster than the diffusive prediction and even faster than a simple exponential, which might be expected if a simple eddy diffusivity were added. § 3 will propose a simple analytic argument to explain this anamolous decay.

3. Single Fourier Mode

For an initial disturbance given by (1), the time evolution can be formally written

as (letting $\theta_0 = 1$)

$$\theta(\vec{r},t) = exp[iqx(t)], \tag{17}$$

where $x(t)$ is the x component of the Lagrangian position of a fluid particle which was at x at time $t = 0$. The amplitude at time t in the initial Fourier mode can be calculated from the inverse Fourier transform

$$A(q,t) = (1/V)\int d\vec{r}\,\theta(\vec{r},t)exp[-iqx]. \tag{18}$$

For homogeneous turbulence the volume integral in (18) averages out the fluctuations and can be replaced by a time or ensemble average. Thus (18) can be formally rewritten as

$$A(q,t) =< exp[iq\{x(t) - x(0)\}] >, \tag{19}$$

where $x(t) - x(0)$ is the Lagrangian displacement of a fluid particle between time 0 and time t. Since the turbulent velocity field is nearly Gaussian, its time integral will be more nearly Gaussian and the central-limit theorem can be applied (Lumley 1970). If $[x(t) - x(0)]$ is a Gaussian random variable, (19) simplifies to

$$A(q,t) = exp[-\frac{1}{2}q^2 w(t)], \tag{20}$$

where

$$w(t) =< [x(t) - x(0)]^2 > \tag{21}$$

is the Lagrangian mean-square displacement. Once it is realized that (19) is the formal expression for the physical quantity of interest, these results are simple and not surprising. Relations similiar to this are common in the analysis of laser-doppler anemometry (Buchave et al. 1978) for time and length scales greater than the turbulent scales. We will show that these relations also provide a means of estimating $w(t)$ for time and length scales below the turbulent scales.

Equations (19) and (20) describe the ensemble average of (17) when all of the Fourier modes, except the excited one, are initially zero. Since the passive-scalar problem is linear, (20) can then be used along with Fourier analysis to describe the average behavior of any initial disturbance. The resulting prescription is to solve the initial-value problem for the ordinary diffusion equation, and then to make the substitution

$$2Dt \rightarrow w(t)$$

at the end to rescale the time behavior.

The Lagrangian mean-square displacement $w(t)$ can be written as

$$w(t) = 2Dt + f(t), \tag{22}$$

where D is the coefficient of molecular diffusion, and

$$f(t) = \frac{1}{3}\int_0^t ds \int_0^t ds' < \vec{u}(\vec{x}(s), s) \cdot \vec{u}(\vec{x}(s'), s') > . \tag{23}$$

In (23) $\vec{u}(\vec{x}(s), s)$ is the velocity of a fluid particle at time s whose position is $\vec{x}(s)$. Since the time domain $s \sim s'$ makes the dominant contribution to the integral, (23) can be approximately rewritten in the form

$$f(t) = \frac{4}{3}\int_0^t ds \int_0^s ds' E(s') h(s, s'), \tag{24}$$

where $E(s)$ is the turbulent kinetic energy per unit mass at time s, and the function $h(s, s')$ represents the decay of correlations. For sufficiently short times $f(t)$ is given approximately by

$$f(t) \approx \frac{2}{3} E(0) t^2. \tag{25}$$

For slightly longer times the decay of correlations can be crudely estimated if we know $E(s)$ and let

$$h(s, s') = exp[-(s - s')/\tau(s')], \tag{26}$$

where $\tau(s)$ is the eddy-turnover time for an energy-containing eddy at time s. If the turbulence were steady both $E(s)$ and $\tau(s)$ would be constant, and our approximation would correspond to a simple Langevin model with $f \sim t$. Since the turbulence is decaying, the result is slightly more complicated, and $f(t)$ is not proportional to t at long times.

4. Comparison to simulation

To get the best comparison with the theory outlined above, we performed the highest Reynolds number simulation possible with a 64^3 grid, a decaying velocity field, and good resolution of the small scales. This is simulation 1. The initial scalar modes, $q_i = 4$, 6, and 8, were picked so as to minimize resolution effects. When plotted semilogrithmically, their time evolution was qualitatively similiar to that in figure 4. A more illustrative manner in which to present their time decay is shown in figure 5. Here

$$f(t) = -\frac{1}{q^2} log(\frac{I(q_i,t)}{I(q_i,0)} - 2Dt, \tag{27}$$

is found directly and plotted. It is seen that all three modes collapse to a single curve up to four times the Kolmogorov timescale, τ_k (13). In fact, the values of $f(t)$ for the three modes agree to two significant figures up to two times τ_k.

If $E(s)$ and $\tau(s)$ are taken from figures 2 and 3, combined with (24) and (26), and numerically integrated, $f(t)$ can be estimated. The theoretically calculated values are plotted as a dashed line in figure 5. For simulation 1, $f(t)$ can be conveniently fitted by the formula $f(t) = 2.1t^{5/3}$, but there is no theoretical significance to this fit. Since the detailed behavior of $f(t)$ depends on the particular energy decay in our simulation and a different energy decay is expected in experiments, the detailed behavior of $f(t)$ will be different in a real flow. However, the procedure followed here should work well for experiments if the turbulence is nearly isotropic.

At $t \approx 4\tau_k$ the calculated value for $f(t)$ for $q_i = 8$ breaks from the other modes and the theoretically predicted curve. To investigate this further we felt it was necessary to investigate modes where the wavenumber was the order of, or greater than, the Kolmogorov cutoff. This was inspired in part by the experiment of Petit & Guyon (1979), whose wavenumber is always the order of, or greater than, k_k. For simulation 1, $k_k \approx 33$, which is the limit to the resolution of a 64^3 simulation. To get good resolution at the higher wavenumbers, it was necessary to reduce the Kolmogorov wavenumber; this could only be done by decreasing the Reynolds number. Therefore, simulation 2 was performed. with $R_\lambda \approx 15$. Besides calculating several wavenumbers, several Prandtl numbers were calculated to see what, if any, effect this had on the calculated value of $f(t)$. The Reynolds number in simulation 2 is similiar to that used in Kerr (1981) on a 32^3 grid, but the additional resolution of the 64^3 grid allows higher scalar wavenumbers to be studied in the current simulation. The simulation in Kerr (1981) of the decay of single scalar modes shows decay similiar to simulation 1.

Figure 6 presents $f(t)$ for all the modes investigated in simulation 2. For short times, the prediction of (24) and (26) is in reasonable agreement with the directly computed value, although the agreement is not as good as for simulation 1. But after about one Kolmogorov timescale it is seen that for the higher modes there is a definite transition to an entirely different decay. This can also be seen for $q_i = 20$ in figure 4. To illustrate this better the region of transition is enlarged in figure 7.

First notice that the time of transition and the subsequent decay are almost independent of Prandtl number for $q_i = 20$ and $q_i = 12$, although the transition for $q_i = 12$ in figure 6 is not shown in figure 7. Recall that the Kolmogorov wavenumber for simulation 2 is 19. For all the modes, even those with $q_i > k_k$, the time of transition is never below $t = \tau_k$, which suggests that this is a lower bound for the transition time. It is also possible that because our maximum wavenumber is only 25% greater than the Kolmogorov wavenumber the transition would occur at ever shorter times if higher wavenumbers could be simulated. Since the only velocity timescale available at the transition is the Kolmogorov timescale, the subsequent decay for all the modes is compared to an exponential of the form $exp(-t/\tau_k)$ for each mode. That is

$$q^2 f(t) = \frac{t}{\tau_k}. \tag{28}$$

Only for $q_i = 24$ does this form seem to follow the subsequent decay closely, but the decay of the other modes would not be inconsistent with a decay of this form. The new decay is not due to the dissipation term in the scalar equation. That contribution has already been subtracted out in (27).

One source for this transition could be numerical error. Very high modes near the resolution of the simulation are simulated and the scalar amplitude in figure 4 has decayed seven orders of magnitude for $q_i = 20$. To check the size of the round-off error simulation 2 was repeated with $q_i = 16, 20$, and 24 for 40 timesteps without packing the 64-bit CRAY words into 32-bit words when doing out-of-core storage on disk. All of the other simulations use packing. No significant differences were seen without packing.

If another source of numerical error were the cause, in particular high-wavenumber truncation error, strong fluctuations would be expected in the amplitude of the initial mode and they would be strongest for $q_i = 24$. All other modes with $|q| \approx q_i$, which were initially zero, would have a similiar amplitude and would also fluctuate. Instead $q_i = 24$ shows the fewest fluctuations. A simulation with $q_i = 27$ was done and it did show strong fluctuations.

Another possibility is that interference occurs when other modes feed their scalar variance back into the original mode. This is undoubtably occurring and is the probable source of the existing fluctuations about a smooth decay. But if it dominated, the sign of the original mode would be expected to change more often and the fluctuations would be greater. Instead, the only times that the mode changes sign are the few major deviations (greater than an factor of two) in the otherwise steady time evolution, and these last only a few timesteps before disappearing. To check the size of the other modes which could feed the original mode, the amplitudes of both the real and imaginary parts of $q_i = 24$ are presented in figure 8. The sharp dips in the imaginary part represent where it changes sign. At the transition, the magnitude of the imaginary part is the same as that of the real part. This might seem large and is reflected to a small degree in the real part, but the frequency of the oscillations is much too large to be connected with the slow decay of the real

part. Even if a feedback mechanism were the dominant source of the new decay, it could be physically significant and might be important in explaining the effect of the envelope shape in the experiments. But we believe that with a large enough sample size, which would require a much larger simulation, the fluctuations caused by other modes feeding the original mode would disappear and that another explanation for the new decay regime exists.

In figure 9 the mixed velocity/scalar derivative skewness

$$S_{u\theta} = \frac{< \frac{\partial u_1}{\partial x_1} (\frac{\partial \theta}{\partial x_1})^2 >}{< \left(\frac{\partial u_1}{\partial x_1}\right)^2 >^{\frac{1}{2}} < (\frac{\partial \theta}{\partial x_1})^2 >} \tag{29}$$

in the direction of the initial wavevector of the scalar is plotted. Kerr (1985) has found that for an isotropic scalar in isotropic, homogeneous turbulence, the mixed skewness will be negative and about -0.5, with some variation, depending on both Reynolds number and Prandtl number in the range considered here. In fact, the mixed skewness in the directions perpendicular to the initial wavevector has this property in the current simulation. However, the mixed skewness in the direction of the initial wavevector has entirely different behavior. Initially, there is no source of correlation between the velocity and scalar, and the mixed skewness is zero. Next, as the scalar begins interacting with the velocity, the mixed skewness becomes negative, much as in Herring & Kerr (1982). Then it starts becoming strongly positive, especially for the higher wavenumber modes. Eventually the mixed skewness peaks and begins decreasing, presumably attaining its isotropic negative value at large enough times.

The manner in which the mixed skewness changes with time appears to be correlated with the transitions in figures 4, 6, and 7. Where the mixed skewness peaks is roughly where the transition to the new decay is observed for each mode. This suggests a strong connection between the new decay rate and correlations containing both the velocity and scalar. Kerr (1985) used models from Tennekes (1968) and Lundgren (1982) to explain some of the correlations he calculated. In these models the small-scale turbulent field is characterized by vortex tubes with large-scale stretching along the tubes and large-scale compression perpendicular to the tubes. Around vortices in the simulations there were, in addition, large values of the rate of strain that were locally induced and did not contribute to turbulence production or to the three-dimensional, kinetic-energy and scalar-variance cascades to large wavenumber. Only the large-scale components of the rate of strain contributed to the cascades, which is why the velocity-derivative skewness (11) and the mixed velocity/scalar derivative skewness (29) were relatively small in the isotropic calculations of Kerr (1985). The negative value of the mixed skewness was explained by the correlation between the strong scalar gradients and the compressive component of the large-scale rate of strain.

In this picture, to get a positive mixed skewness, as in figure 9, there must be scalar fluctuations correlated with the large-scale stretching, hence along the vortices. We propose that these scalar fluctuations eventually dominate the scalar field because of selective decay. In Kerr (1985), the strongest velocity gradients, and hence the maximum dissipation of the scalar, were perpendicular to the vortices. This suggests that regions of the initial scalar mode which are perpendicular to vortices will disappear the soonest. This is demonstrated in figure 10a. Since these are the fluctuations that would contribute to a negative mixed skewness, eventually the only fluctuations remaining are along the vortices, that is those that would contribute to a positive mixed skewness. These are shown in figure 10b. Thereafter, the dynamics of isotropic turbulence begin to dominate and the mixed skewness becomes more negative.

The time it takes until the fluctuations along vortices dominate in figure 9 is one Kolmogorov timescale. Since this is found when the wavenumber of the initial mode is high and when the timescale of the decay of the fluctuations perpendicular to vortices is short, it implies that there must be few fluctuations along vortices, which implies that the vortices are highly aligned and supports Kerr (1985). After this the only mechanism by which the scalar can become decorrelated with the velocity and for there to be more decay, is for the velocity field to change and the vortices to move. For the smallest scales this occurs on the Kolmogorov timescale, which is the timescale of the decay of the scalar after the transition.

For scalar modes with wavenumber much less that the Kolmogorov wavenumber, such as in simulation 1, the same dynamics are expected to apply, but not as strongly. Because the length scale of the initial scalar disturbance is much greater than the scale of the dissipation structures in the velocity field, the scalar fluctuations should selectively align along structures larger than the dissipation structures. The timescale on which this would happen would be associated with the timescale of these larger structures. The numerical results suggest that $q^2 f(t)$ is always about 10 at the transition (Table 1), or that the magnitude of the initial mode at the transition is always nearly the same. This might provide a means of predicting when the transition will occur in experimental flows.

To see how the scalar which was in the initial mode spreads into the other modes, the one-dimensional scalar-variance spectrum in the direction of the initial mode is given in figure 11 for simulation 2 and $q_i = 16$. At later times the spectral peak has moved from the band containing the initial mode to lower wavenumber bands. This occurs well before the transition and a distinct spectral regime should also be noted. A $k^{-5/3}$ line is drawn for comparison. The three-dimensional variance spectrum and the one-dimensional spectra in the other directions do not show such distinctive behavior.

5. Relation to Experiment

In applying (4) to experiment the envelope function should be evaluated at the time-evolved position $\vec{r}(t)$ rather than at $\vec{r}$. In addition, an actual detector

will see the scalar intensity in a band of wavenumbers rather than exactly at the initial wavenumber. Despite these oversimplifications some useful conclusions can be drawn. Equation (4) can be formally rewritten in the form

$$I(q,t) = \int d\vec{r}_1 \int d\vec{r}_2 S(\vec{r}_1)S(\vec{r}_2) < exp[iq(x_1(t) - x_1 + x_2 - x_2(t))] > \quad (30)$$

In this form it is clear that the measured intensity depends on the turbulent diffusion of a pair of fluid particles.

However, there is one limit in which this expression simplifies considerably. Suppose that the width l of the envelope function in any direction is large compared to the integral length scale L of the turbulence, and suppose further that the turbulence is homogeneous. Then the envelope function becomes irrelevant, and the volume integral in (4) extends over a sufficient range to average out the turbulent fluctuations. The ensemble average in (4) becomes superfluous and reduces to

$$I(q,t) = A^2(q,t), \quad (31)$$

where $A(q,t)$ is given by (19). Now the diffracted intensity is directly related to the single Fourier mode problem of § 3,4. The same result can be seen from (30). Under these conditions the main contribution to the double integral comes from trajectories $x_1(t)$ and $x_2(t)$ that are separated by a large distance compared to L. The motion of fluid particles 1 and 2 in (30) is then uncorrelated, and the exponential in (30) can be factored. The essential observation is that this factorization depends on the scale l of the envelope function, and not on the much smaller scale q^{-1} of the periodic pattern.

If l becomes comparable to the integral length scale L, (30) must be looked at more closely. As a first approximation we continue to assume that the two-particle displacement

$$\varsigma_{12}(t) = x_2(t) - x_2 - x_1(t) + x_1 = \delta x_2(t) - \delta x_1(t) \quad (32)$$

is a Gaussian random variable. Equation (30) can then be written as

$$I(q,t) = \int d\vec{r}_1 \int d\vec{r}_2 S(\vec{r}_1)S(\vec{r}_2) exp[-\frac{1}{2}q^2 w_{12}(t)] \quad (33)$$

where

$$w_{12}(t) = < [\varsigma_{12}(t)]^2 > = w_1(t) + w_2(t) - 2 < \delta x_2(t)\delta x_1(t) > \quad (34)$$

For homogeneous turbulence, $w_1(t)$ and $w_2(t)$ do not depend on position, but the correlation term in (34) is a function of the initial separation. Equation (34) then becomes

$$I(q,t) = exp[-q^2 w(t)] \int \int d\vec{r}_1 d\vec{r}_2 S(\vec{r}_1)S(\vec{r}_2) exp[+q^2 < \delta x_2(t)\delta x_1(t) >] \quad (35)$$

This can be simplified further at short times. The exponent in the integrand will go as t^2 times the correlation in velocity between points 1 and 2 at time zero, but this does not allow an explicit integration. Whatever the initial separation of the pair of particles, they will eventually diffuse in an uncorrelated way, so that at long enough times the correction term in (35) will vanish. Thus we expect a correction for correlated pair diffusion which increases $I(q,t)$ over the single-mode result at short times, but which vanishes at long times. In principle, if the experiments meet these conditions, the theory and simulations of § 3,4 should apply. In practice, experimental detectors are never ideal and corrections to our theory would be necessary in order to make proper comparisons.

In Petit & Guyon (1979) and later experiments, the wavenumber of the initial mode is between the Kolmogorov and Batchelor cutoffs, the Prandtl number is high, and the time regime is between the Kolmogorov timescale and the large-scale eddy-turnover time. Simulation 2 is an attempt to simulate a regime like this. In more recent experiments, Limat (1984) finds that the decay obeys $exp(-t/\tau)$ and that by removing the contribution of the diffusive decay a turbulent decay time τ_t can be found, where $1/\tau = 1/\tau_D + 1/\tau_t$ and $1/\tau_D = q^2 D$. That is, similiar to (28),

$$\frac{t}{\tau_t} = q^2 f(t).$$

Table 2 shows the dependence of the ratio τ_t/τ_k on Reynolds number in Limat's experiment along with the Kolmogorov length and timescales. There is no dependence on the wavelengths of the initial modes, $p = 2\pi/q$, which are given in Table 3. The order of magnitude of τ_t/τ_k is one, which is consistent with our second decay regime. If the turbulent timescale depended only on τ_k, then τ_t/τ_k should be constant. Table 2 shows that it is not, but its variation with Reynolds number is consistent with the effect of the envelope width. What should be compared to find the effect of the envelope is not $\Delta q/q = l^{-1}/q$ as in Limat (1984), but $l^{-1}/k_k = \eta/l$. That is, the dimension of the mixing structures must be small compared to the width of the envelope to minimize interference between modes, which would in turn increase the decay rate. Table 3 shows the experimental wavelength, the dispersion of the envelopes, and their width. Notice that l is constant. Therefore, since both the fundamental decay and the width of the envelope are independent of wavenumber, the experimental decay rates should be independent of wavenumber. The only effect on τ_t/τ_k from the envelope will be due to changes in η, which decreases with Reynolds number. As η decreases, the interference between modes will decrease, the decay will decrease, and τ_t/τ_k will increase. Therefore, τ_t/τ_k will increase with Reynolds number. From Table 2, which gives η/l and τ_t/τ_k, we find that

$$\frac{\tau_t}{\tau_k} = 0.7 - 1.5\frac{\eta}{l}. \tag{36}$$

For infinite Reynolds number or infinite envelope size, this predicts that $\tau_t = 0.7\tau_k$, which is consistent with our calculations. Therefore we find excellent agreement between the experiment and our simulation.

It would be interesting if the experiments could show a transition similiar to the one in our calculations. This could be done by making measurements closer to the time that the initial mode was imposed, increasing the Kolmogorov timescale by reducing the turbulence intensity, or by decreasing the wavenumber of the initial mode. If the transition were observed, it could provide important new information on the structure of small-scale turbulence.

6. Relation to practical problems

Would either the initial decay of the single mode or the decay after the transition have an important effect on our understanding of most turbulent dispersion? Certainly they would not have a strong effect on decay of large-scale fluctuations over large timescales. Even for length scales within the turbulent flow, the scalar fluctuations would decay so completely before the transition occurred that the transition would not be observed except in the few special cases where a single mode can be imposed. Besides the experiment of Petit & Guyon (1979) there might be some applications in laser doppler anemometry. For a sharp scalar profile in physical space, such as the temperature-interface problem of Larue & Libby (1981), the only effect might be a slightly enhanced initial turbulent diffusivity. In most practical applications it is difficult to separate the initial scalar profile from the large scale velocity field, and the regimes discussed here would not apply.

We would like to thank M. Cloitre and E. Guyon for useful conversations concerning the relation between the calculations performed here and their laser experiment. We are grateful to L. Limat for sending his thesis. The work of two of the authors (M.N. and T.N.) was supported by the National Science Foundation under grant number MEA 79-02942.

REFERENCES

Batchelor, G.K. 1959 Small-scale variation of convected quantities like temperature in turbulent fluid. Part 1. J. Fluid Mech. 5, 113-133.

Buchave, P., George, W.K. Jr., Lumley, J.L. 1979 The measurement of turbulence with the laser-doppler anemometer. Ann. Rev. Fluid Mech. 11, 443-503.

De Gennes, P.G. 1977 Principe de nouvelles mesures sur les ecoulements par echauffements optiques localises. J.de Physiques 38, L-1.

Fermiger, M., Cloitre, M., Guyon, E. & Jenffer, P. 1982 Utilisation de la diffusion Rayleigh forcee a l'etude d'ecoulements laminaires et turbulents. J. de Mecanique theorique et appliquee, 1, 123-146.

Herring, J.R. & Kerr, R.M. 1982 Comparison of direct numerical simulations with predictions of two-point closures for isotropic turbulence convecting a passive scalar. J. Fluid Mech. 118, 205-219.

Kerr, R.M. 1981 Theoretical investigation of passive scalar such as temperature in isotropic turbulence. Ph.D. thesis; Cooperative thesis no. 64, Cornell Univ. and Nat. Center for Atmospheric Res.

Kerr, R.M. 1985 Higher-order derivative correlations and the alignment of small-scale structures in isotropic, numerical turbulence. J. Fluid Mech. 153, 31-58. (see also NASA TM 84407, 1983)

Larue, J.C. and Libby, P.A. 1981 Thermal mixing layer downstream of half-heated turbulence grid. Phys. Fluids 24, 597-603.

Limat, L., Thèse de troisième cycle, Ecole superieure de physique et de chemie industrielles de la ville de Paris, 1984.

Lumley, J.L. 1970 Stochastic Tools in Turbulence. Academic Press, New York.

Lundgren, T. S. 1982 Strained spiral vortex model for turbulent fine structure. Phys. Fluids 25, 2193-2203.

Petit, L. & Guyon, E. 1979 Sur une nouvelle methode d'etude de la diffusivite turbulente. J. de Physique 40, 1207-1217.

Rogallo, R. 1981 Numerical experiments in homogeneous turbulence. NASA TM 81315.

Tennekes, H. 1968 Simple model for the small-scale structure of turbulence. Phys. Fluids 11, 669-671.

Tennekes and Lumley 1972 A First Course in Turbulence. Cambridge: MIT Press.

Warhaft, Z. & Lumley, J.L. 1978 An experimental study of the decay of temperature fluctuations in grid-generated turbulence. J. Fluid Mech. 88, 659-684.

Table 1: Velocity scales, scalar parameters (Prandtl number and wavenumber) and the transition parameter $q_i^2 f(t)$ for the two simulations.

Simulation 1			
Trials	$R_\lambda = 45$	$k_k = 33$	$\tau_k = 0.046$
Pr	0.7	0.7	0.7
q_i	4	6	8
$q_i^2 f(t)$			7.8

Simulation 2							
Trials	$R_\lambda = 15$		$k_k = 19$		$\tau_k = 0.086$		
Pr	0.7	0.7	4.0	4.0	4.0	4.0	4.0
q_i	12	20	12	16	20	22	24
$q_i^2 f(t)$	9.6	10.2	9.6	9.6	10.2	8.4	10.9

Table 2: Experimental time and length scales and appropriate ratios from Limat (1984). The envelope length scale l is assumed to be 275μ for all the experiments (see Table 3).

Re	2300	3800	6840
$\eta_B(\mu)$	15	10	8
$\eta_k(\mu)$	70	50	35
τ_k	3400	1700	800
τ_T/τ_k	0.3	0.4	0.5
η_k/ℓ (ℓ = 275 μ)	0.25	0.18	0.13

Table 3. Experimental wavelengths, the dispersion of the envelopes, and the widths of the envelopes from Limat (1984).

P (μ)	30	50	85	100
$\delta q_o/q_o$	0.11	0.18	0.31	0.36
$\ell = P\left(\frac{\delta q_o}{q_o}\right)^{-1}$ (μ)	272	277	274	277

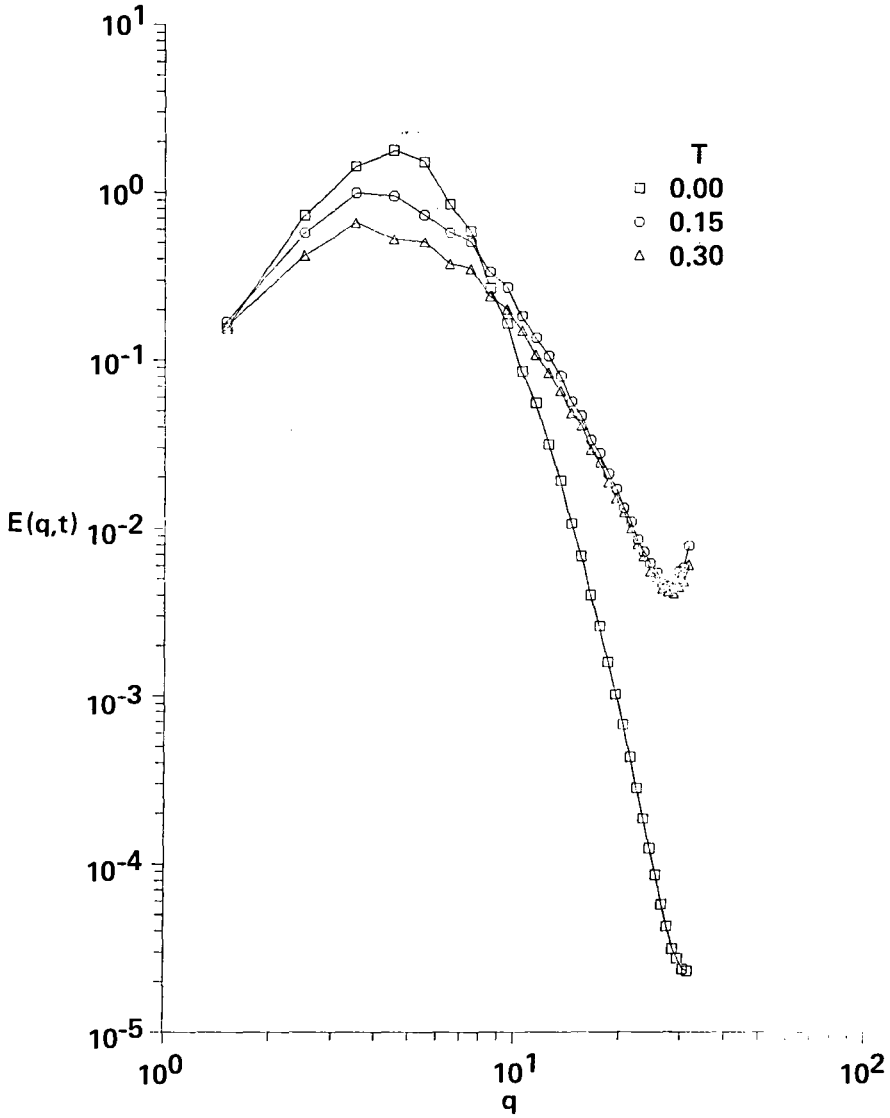

Figure 1: Kinetic-energy spectra for three times from simulation 1, a 64^3 simulation of decaying, isotropic turbulence whose initial spectrum was $q^4 exp(-q^2)$ with a peak at $q = 4$. $t = 0$ is when the velocity-derivative skewness (11) $S_u \approx -0.4$ and the scalar fluctuations are introduced. $R_\lambda = 45$ at $t = 0$. Square: $t = 0.0$. Circle: $t = 0.15$. Triangle: $t = 0.30$.

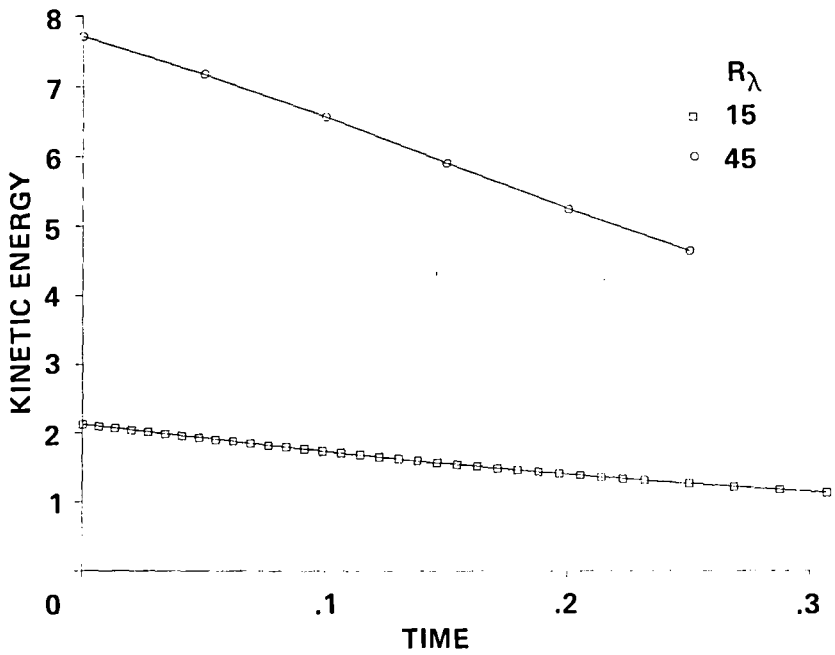

Figure 2: The decay of kinetic energy E with time for simulations 1 (circle) and 2 (square).

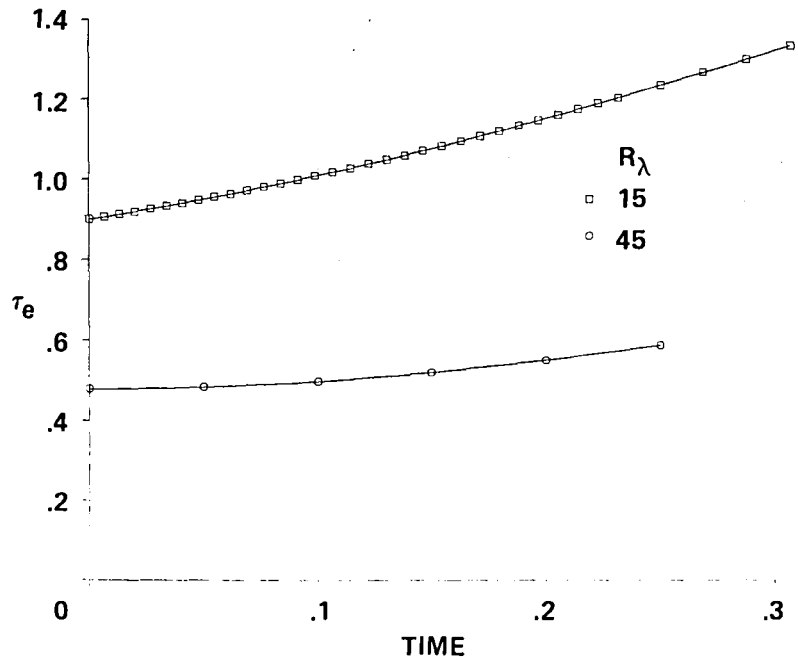

Figure 3: The eddy-turnover time τ_e (14) as a function of time for simulations 1 (circle) and 2 (square).

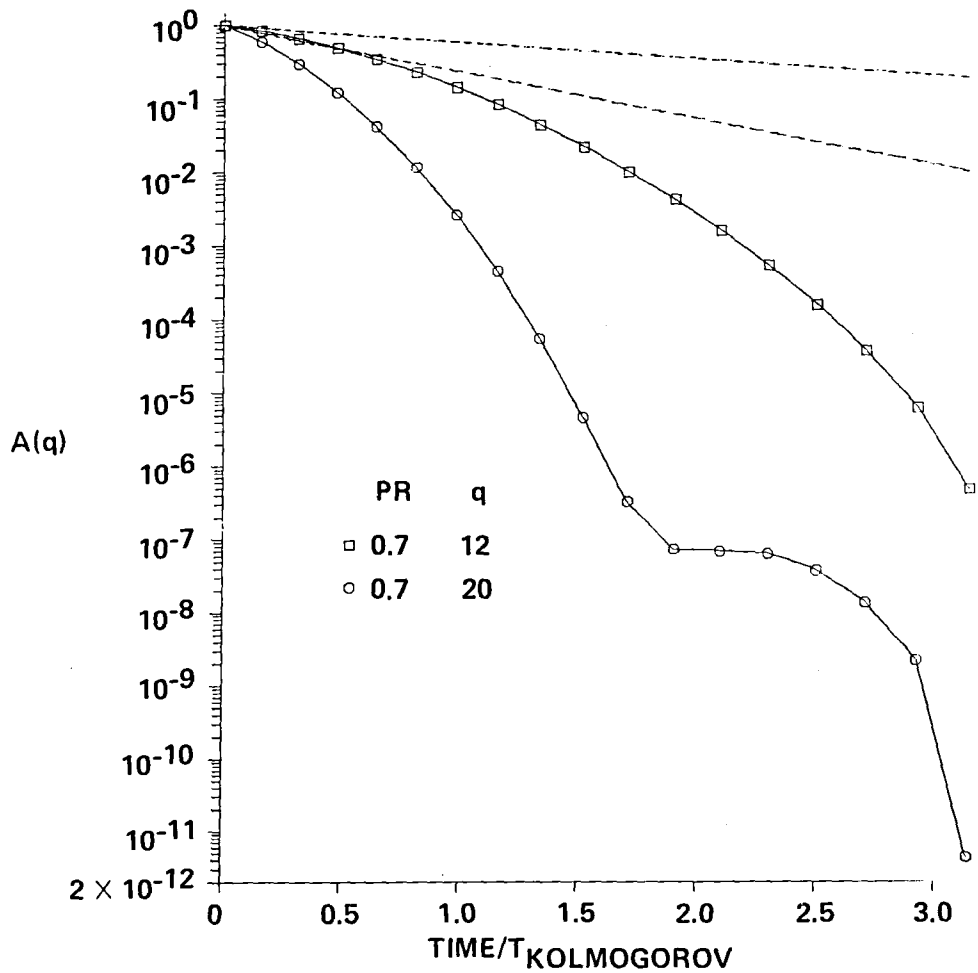

Figure 4: The amplitude $A(q,t)$ of an initially coherent, passive-scalar disturbance with spatial dependence $cos(qx)$ plotted as a function of time for two cases from simulation 2. Square: $Pr = 0.7$, $q = 12$. Circle: $Pr = 0.7$, $q = 20$. The dashed lines represent purely diffusive decay for the two cases.

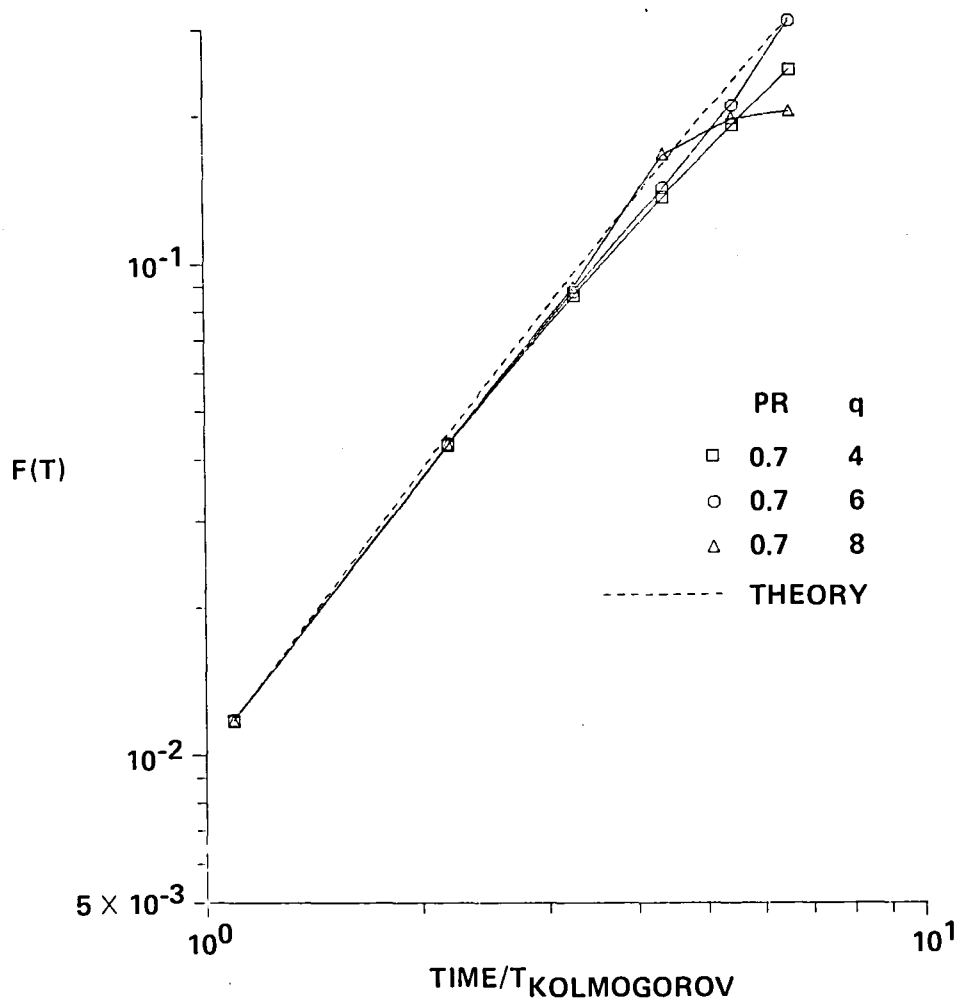

Figure 5: $f(t)$ (27) plotted as a function of the Kolmogorov normalized time for three cases from simulation 1 ($R_\lambda = 45$). Square: $Pr = 0.7$, $q = 4$. Circle: $Pr = 0.7$, $q = 6$. Triangle: $Pr = 0.7$, $q = 8$. The agreement of all three wavenumbers to $t = 3\tau_k$ indicates that the Gaussian approximation is accurate for short times. The dashed curve is from the Lagrangian theory of § 3 (24). The apparent power-law fit of the theory has no theoretical significance. Note that $q = 8$ diverges strongly from the theory after $t = 4\tau_k$.

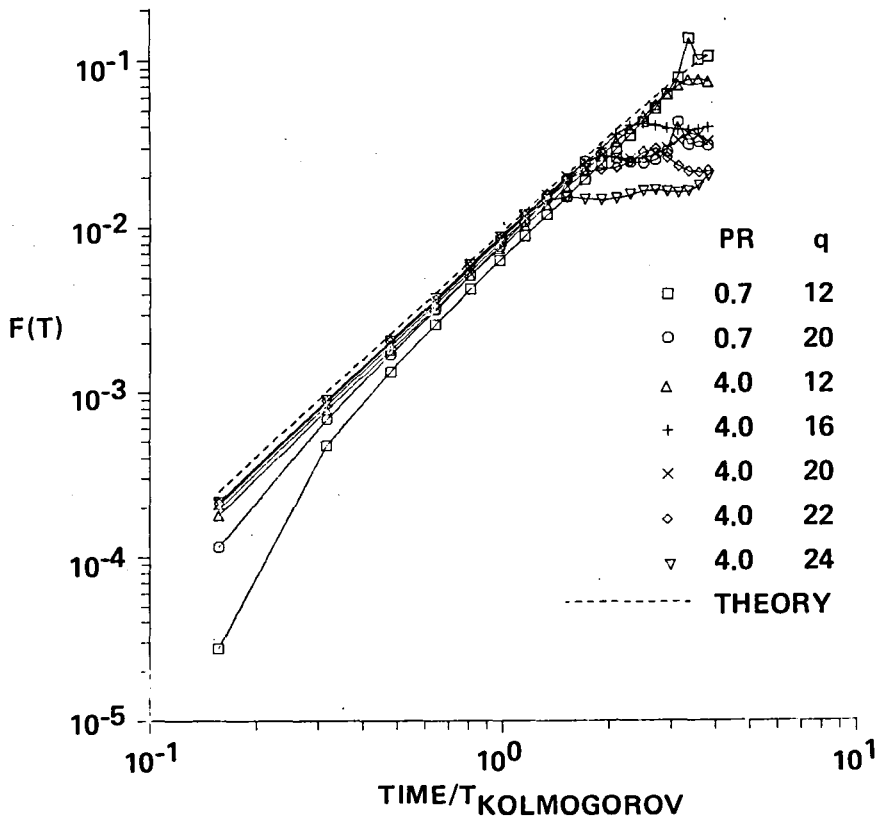

Figure 6: $f(t)$ (27) plotted as a function of the Kolmogorov normalized time for seven cases from simulation 2 ($R_\lambda = 15$). Square: $Pr = 0.7$, $q = 12$. Circle: $Pr = 0.7$, $q = 20$. Triangle: $Pr = 4.0$, $q = 12$. Plus: $Pr = 4.0$, $q = 16$. Cross: $Pr = 4.0$, $q = 20$. Diamond: $Pr = 4.0$, $q = 22$. Inverted triangle: $Pr = 4.0$, $q = 24$. The relatively poor convergence at early times is probably due to the low Reynolds number of the simulation. Above $t = \tau_k$ the decay diverges from the Lagrangian theory (24), represented by the dashed line, in each case, diverging soonest for the highest wavenumbers.

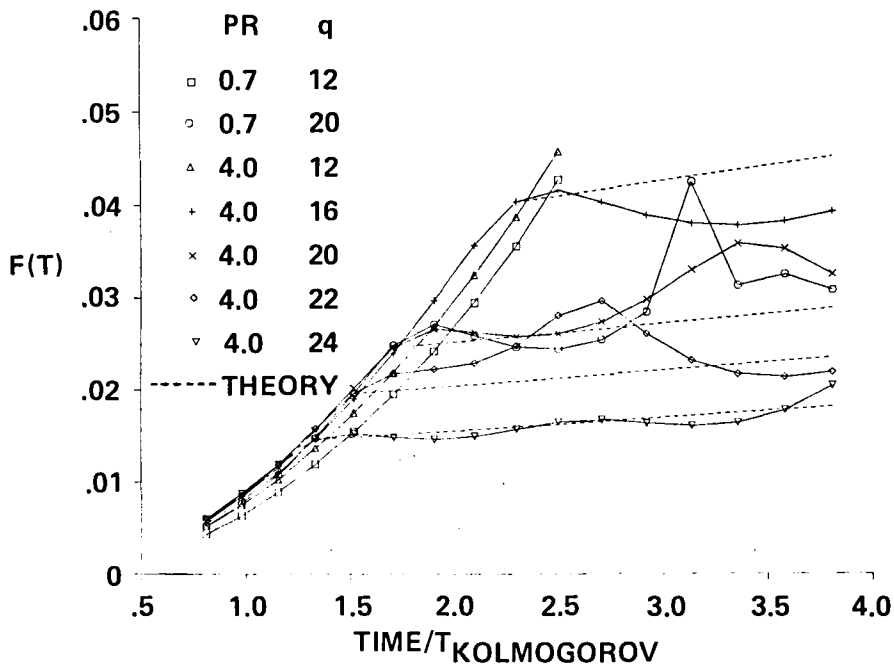

Figure 7: From figure 6, f(t) enlarged for $t > 0.8\tau_k$. The major discontinuity for $Pr = 0.7$, $q = 20$ is where the value of the initial mode is temporarily negative. The dashed lines are exponential decays associated with the Kolmogorov timescale, $exp(-t/\tau_k)$.

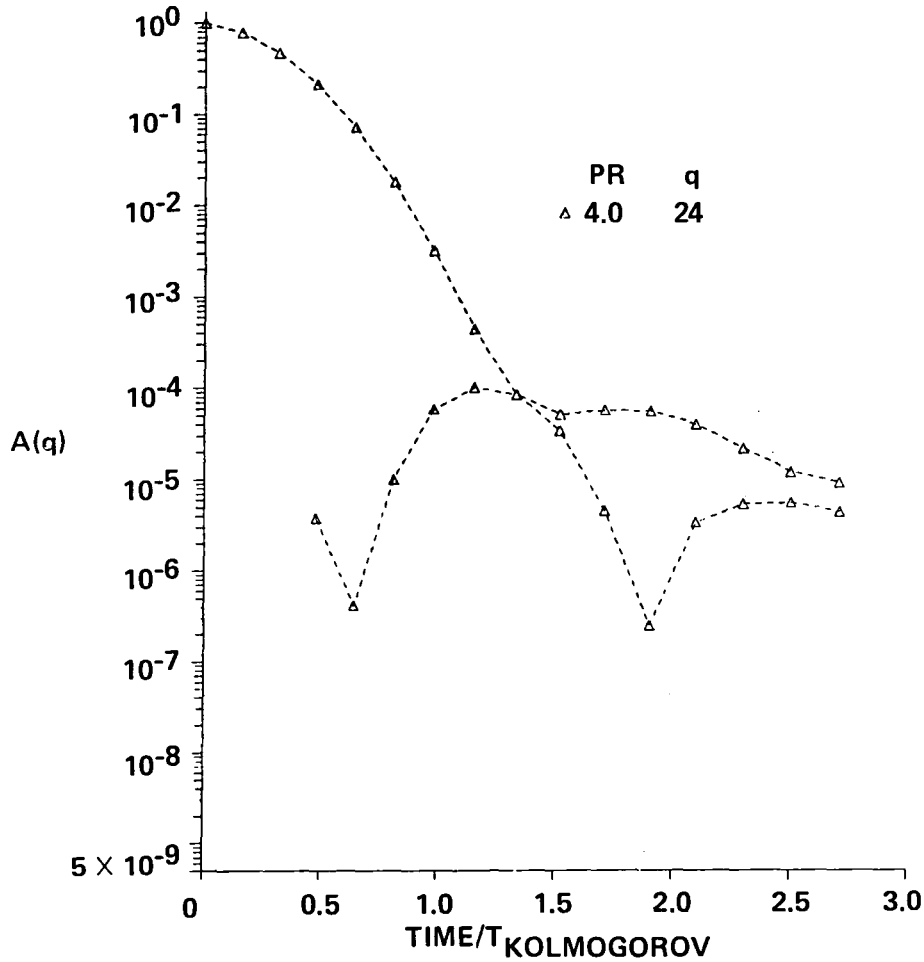

Figure 8: Amplitudes of the real (upper curve) and imaginary (lower curve) parts of the initial mode for $Pr = 0.7$, $q = 24$ as functions of the Kolmogorov normalized time. The major discontinuities in the imaginary part are where it changes sign.

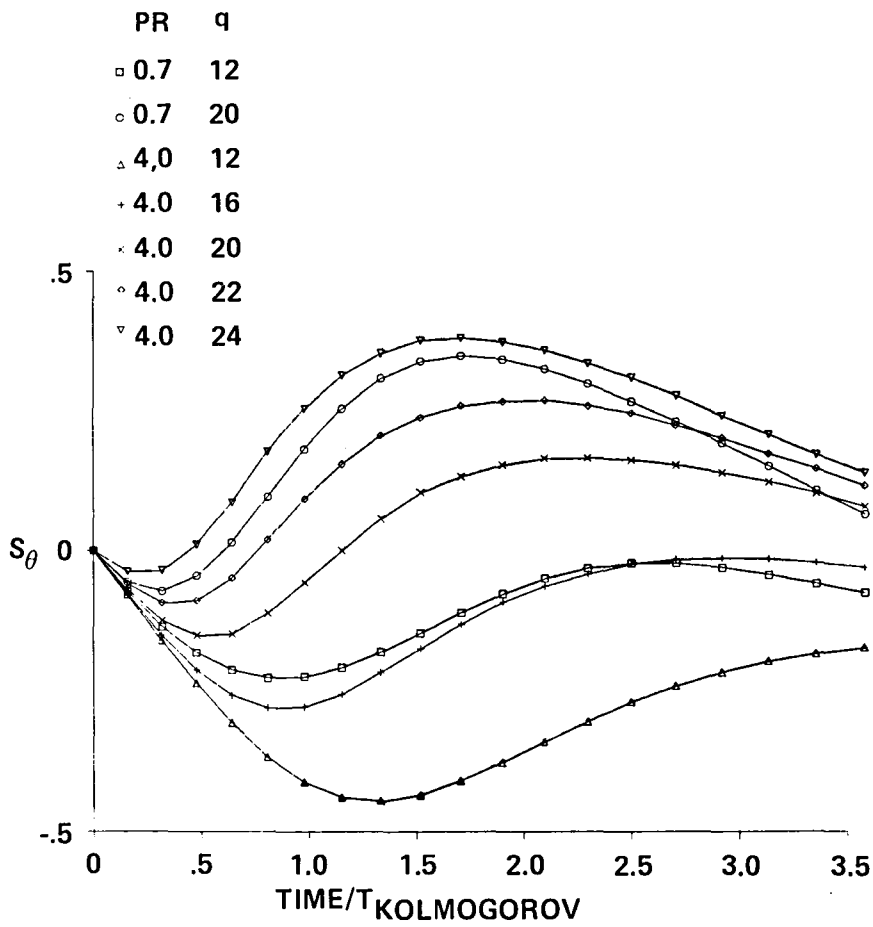

Figure 9: The mixed velocity/scalar derivative skewnesses $S_{u\theta}$ (29) from simulation 2 as functions of the Kolmogorov normalized time.

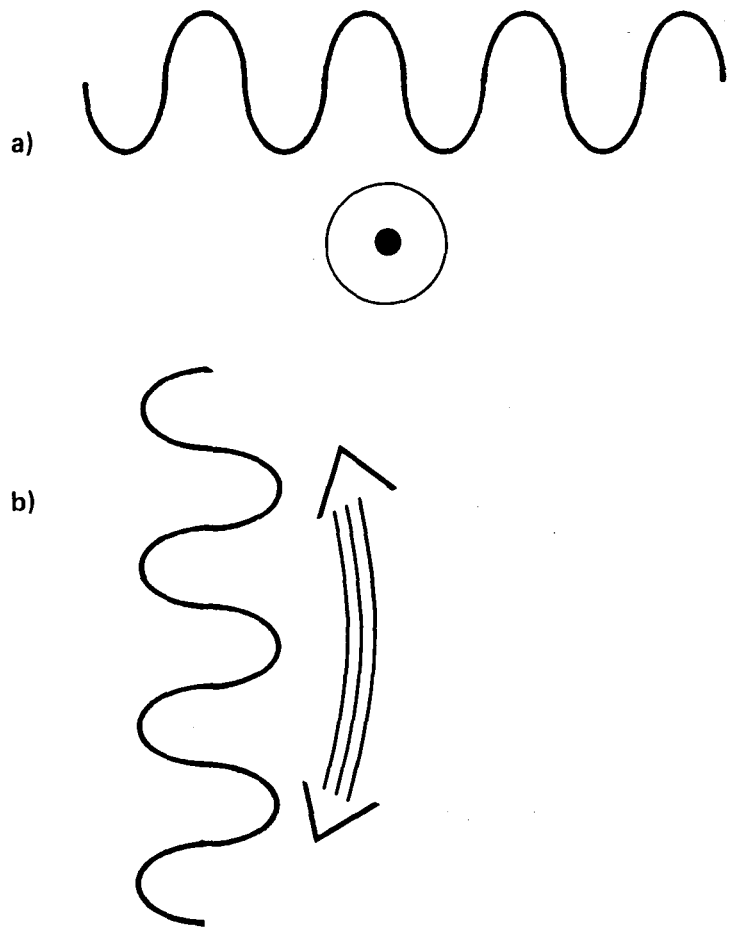

Figure 10: How scalar fluctuations can align with the voriticity. Hypothetical scalar fluctuations are shown by sine waves. a: Looking at a three-dimensional vortex from the top down. The arrow indicates a streamline. The wavenumber of the scalar fluctuation is perpendicular to the vorticity. b: Looking at three-dimensional vortex from the side. The arrow indicates vortex stretching. The wavenumber of the scalar fluctuation is parallel to the vorticity.

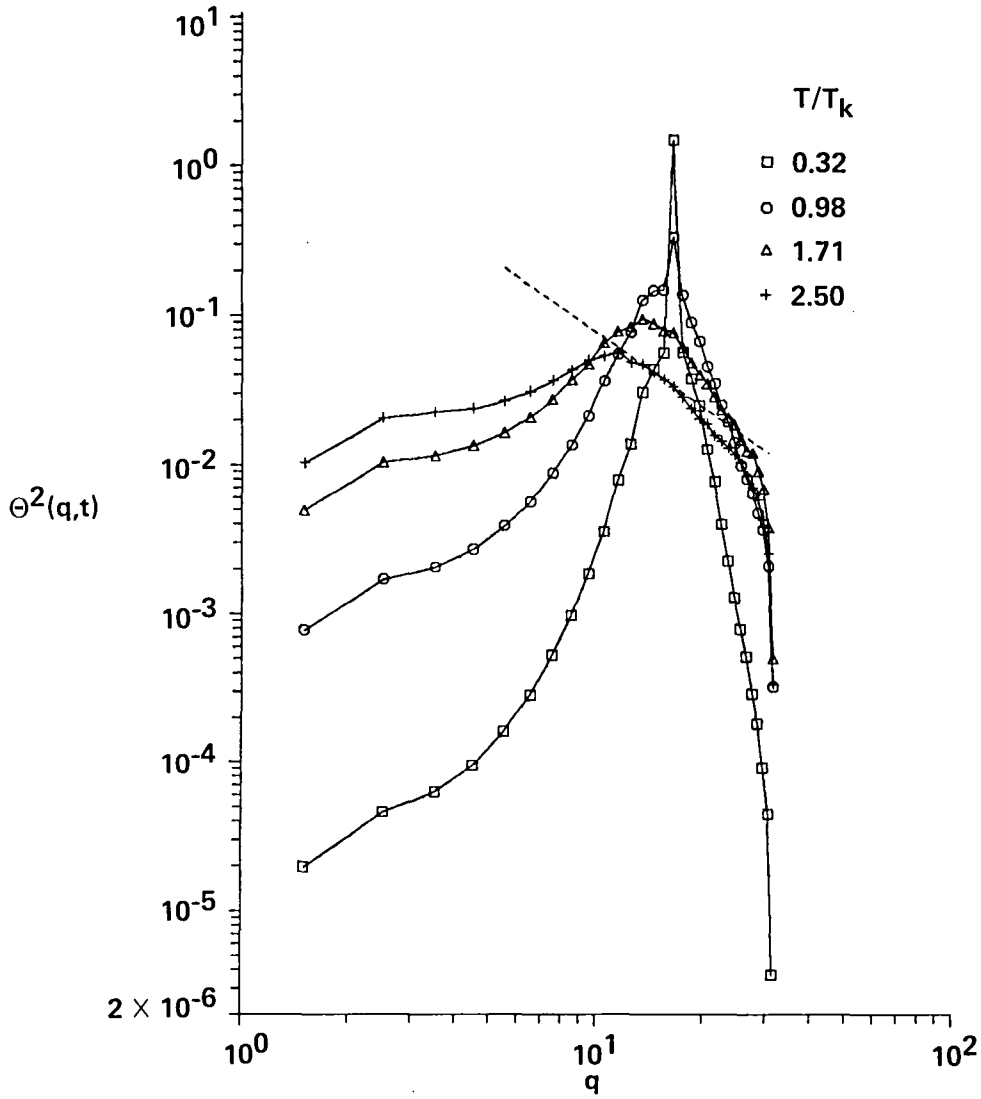

Figure 11: One-dimensional scalar-variance spectra $E_\theta(k_1)$ in the direction of the initial mode from simulation 2 for $Pr = 4.0$, $q = 16$. The time is with respect to where $S_u \approx -0.4$. Square: $t/\tau_k = 0.32$. Circle: $t/\tau_k = 0.98$. Triangle: $t/\tau_k = 1.71$. Plus: $t/\tau_k = 2.50$. The dashed line represents a $k^{-5/3}$ spectrum.

1. Report No.	2. Government Accession No.	3. Recipient's Catalog No.
NASA TM-86700		

4. Title and Subtitle	5. Report Date
DECAY OF A COHERENT SCALAR DISTURBANCE IN A TURBULENT FLOW	June 1985
	6. Performing Organization Code
7. Author(s)	8. Performing Organization Report No.
Robert M. Kerr, Tohru Nakano, and Mark Nelkin	85161
	10. Work Unit No.
9. Performing Organization Name and Address	
Ames Research Center Moffett Field, CA 94035	11. Contract or Grant No.
	13. Type of Report and Period Covered
12. Sponsoring Agency Name and Address	Technical Memorandum
National Aeronautics and Space Administration Washington, DC 20546	14. Sponsoring Agency Code 505-31-01-01-00-21

15. Supplementary Notes

Point of contact: Harvard Lomax, Ames Research Center, MS 202A-1, Moffett Field, CA 95035, (415)694-5124 or FTS 464-5124

16. Abstract

The time evolution of an initially coherent, sinusoidal passive-scalar disturbance is considered when the wavelength q is less than the length scale of the surrounding isotropic turbulent flow. In 64^3 direct numerical simulations a Gaussian prescription for the average scalar amplitude breaks down after a timescale associated with the wavenumber of the disturbance and there is a transition to a new characteristic decay. The Gaussian prescription is given by $\exp[-(1/2)q^2w(t)]$, where a form for $w(t)$, the Lagrangian mean square displacement of a single fluid particle, is proposed. After the transition the decay is given by $\exp[-t/\tau]$, where τ is the new characteristic timescale. If $q > k_k$, then $1/\tau = 1/\tau_D + 1/\tau_k$, where k_k is the Kolmogorov wavenumber, τ_D is the diffusive timescale and τ_k is the Kolmogorov timescale. For $q < k_k$, there is a transition, but the new decay has not been characterized.

An experiment originally proposed by de Gennes is considered in which the evolution of a coherent laser-induced pattern is read by a diffracting laser. The theory of this experiment involves the dispersion of particle pairs, but it is shown that in a certain limit it reduces to our single Fourier-mode problem and can be described in terms of single particle diffusion. The decay of a single mode after the transition in the simulation best describes the experiment.

17. Key Words (Suggested by Author(s))	18. Distribution Statement
Turbulence Numerical simulation Mixing Chaos Statistical physics	Unlimited Subject category - 34

19. Security Classif. (of this report)	20. Security Classif. (of this page)	21. No. of Pages	22. Price*
Unclassified	Unclassified	32	A03

*For sale by the National Technical Information Service, Springfield, Virginia 22161

End of Document